SUBFRAME

Subsea Underwater Buoyancy and Frame Research for Artificial reefs and Monitoring Engineering

IUC characteristic: 202503107
Date: 26/02/26
Version: Final

Financed by:

Natuurversterking NOORDZEE

Funded by the European Union
NextGenerationEU

Project partners:

Seaward

WATER PROOF

De Rijke Noordzee

Justification

Title:	SUBFRAME
Subtitle:	Subsea Underwater Buoyancy and Frame Research for Artificial reefs and Monitoring Engineering
Client:	Nature Regeneration North Sea
Project #:	202503107
Version:	03 - final
Date:	26/02/26
Main author:	Frank Jacobs (Seaward) 
Co-authors:	Nathanaël Geleynse (WaterProof), Kamiel Roëll (WaterProof)
With thanks to:	Isaac de Boer-Ferrier (The Rich North Sea) Sam Hidskes (Min. LVVN) Luca van Duren (Deltares)
Contact details:	frank@seaward.blue

Contents

Nederlandse samenvatting

Voor het Natuurversterking Noordzeeprogramma Noregret SUBFRAME is een rekentool ontwikkeld om snelle ontwerpiteraties mogelijk te maken voor onderwaterconstructies en hun stabiliteit.

De tool, die geprogrammeerd is in Python, levert stabiliteitsresultaten die binnen 20% van een gedetailleerde berekening liggen. Over het algemeen geeft een onzekerheidsmarge van 20% een goede orde-grootte schatting van de stabiliteit van de constructie.

Deze 20% onzekerheid is lager bij eenvoudige en gesloten constructies en neemt toe bij open constructies.

De tool is gebaseerd op de Morison-vergelijkingen, maakt gebruik van lineaire golftheorie (Airy-wave) en kan eenvoudige of gereduceerde (versimpelde) mesh 3D-objecten laden voor snelle iteraties.

Het rapport beschrijft verder ontwerpoverwegingen, bijvoorbeeld het reduceren van de mesh en het verschil tussen discrete en single-point stroomberekeningsmethoden.

Er wordt een vergelijking gemaakt met de methodologieën van WaterProof en de rekenmethode die is toegepast in het ECOFRIEND-project. Over het algemeen levert de hier voorgestelde SUBFRAME-methodologie goede resultaten op qua orde van grootte.

Verbeteringen van het programma liggen met name in meer opties, rekenopties en resultaatopties. De belangrijkste verbeterpunten zijn:

- Handmatige inputs voor berekende waarden, zoals het zwaartepunt (COG).
- Sneller 3D-meshes inlezen, aangezien de tool nu een vereenvoudigde mesh vereist
- Het opslaan van een berekening.

In de toekomst kan extra functionaliteit worden toegevoegd, zoals de optie voor Monte Carlo-simulaties die door middel van veel berekeningen limieten van de structuur onder verschillende omstandigheden weergeeft, en de mogelijkheid om twee of meerdere ontwerpen qua stabiliteit met elkaar te vergelijken.
Er zijn stappen in deze richting gezet, maar om de ontwikkeling van de software verder uit te werken en te valideren moet een vervolgproject worden overwogen.

Deze rekentool is momenteel een eerste stap naar complete software die uiteindelijk kan worden gebruikt voor snelle iteraties, gevalideerd en geverifieerd is en geaccepteerd wordt door bijvoorbeeld windparkbeheerders, omdat deze gebaseerd is op fundamentele berekeningsprincipes.

Executive summary

A calculation tool was developed to make quick design iterations possible for underwater structures and their stability. The tool, using Python software, is assumed to offer stability results within 20% of a detailed calculation. In general, taking 20% uncertainty margin gives a good estimate of structure performance. This uncertainty is lower with more simple and closed structures and increases with open structures.

The tool is constructed based on the Morison equations, uses linear wave theory (Airy waves) and can load simple or reduced mesh 3D objects for quick iterations. Further, the report details design considerations such as discrete and singe point current calculation methods.

A comparison is made with the methodologies used by WaterProof, which works on a case-by-case basis, and the calculation methodology applied to the ECOFRIEND project. In general, the SUBFRAME methodology proposed here gives good order-of-magnitude results and can be improved to have more options, calculation options and output options.

Main improvement points would be the manual override setting on every calculated value, such as COG. faster 3D mesh loading, as the tool now requires either long wait times or a reduced (simplified) mesh, and saving of a calculation.

Additional functionality may be programmed in the future, such as the option for Monte Carlo simulations giving detailed limits of the structure in various conditions, and the option to compare two designs with each other in terms of stability. Steps were made in this regard but in order to validate the methodologies a follow-up project might be considered.

This calculation tool as of now is a first step into a complete software which ultimately might be used for quick iterations, is validated and verified, and accepted by e.g. wind farm operators as it is based on first-principle calculation bases.

1 Introduction

1.1 Background

With the rise in offshore windfarms (OWFs) in the Dutch North Sea and more and more ecological considerations from the Dutch Ministry of Agriculture, Nature and Food Quality with respect to new offshore wind tenders such as Nederwiek and Doordewind, the placement of artificial reefs and source populations of reef builders such as European flat oyster is increasing.

Until recently, a clear prediction method of structure or species stability on the seabed was carried out by integrating inhouse developed scripts and doing flume tests on scale models to assess stability.

In the Joint-Industry-Project ECO-FRIEND experimental and numerical modelling was carried out on an oyster restoration project in windfarm Gemini. A basic stability model of the used oyster cages was created, based on the general applicable Morison equation for submerged structures. The Morison equation determines wave forces on structures, consisting of inertia and drag force components that require coefficients dependent on the Keulegan-Carpenter and Reynolds numbers.

When structures are to be placed on or near the seabed, some challenges with predicting performance and stability of these structures arise:

- Modelling, detail of model and material properties
- Placement, is it fully horizontal, does the structure sink into the seabed?
- Soil and seabed characteristics at a local level (deployment location)
- Availability of environmental data, such as near-bed orbital and current velocities during storm conditions
- Time-dependent issues such as sanding over time
- Assumptions of model (frontal current, assumptions of coefficients Cm, Cd, Reynolds, Keulegan-Carpenter)

1.2 Goals

This Nature Regeneration North Sea project aims to bring the knowledge about stability assessments a step further, by aiming to complete the following goals:

- Pinpointing the strengths and weaknesses of the ECO-FRIEND model, pointing out possible improvements and/or areas of caution when using the equations for real-life deployments in the field.
- Investigation of applicability for case studies (e.g., Ecofriend and WINOR cases) and providing advice for improvements in the stability calculation process.
- Provide advice on how to approach a stability study, and making this available to experts.
- Disseminate learned lessons regarding stability and 'real life' situations to increase the success rate of practical experiments and enable the safe and stable scaling up of artificial structures.

2 Approach

2.1 Introduction

In this chapter we start with collecting data on known deployed structures that have been placed in offshore wind farms, collecting specifications such as dimensions, weight and deployment duration. We see if there is any stability calculation information: was there one carried out and if yes, which method(ology) was used? Further we assess structure displacement incidents, did the structure move or disappear or got sanded over?

In chapter 3 we explain the theory and considerations that have to be taken into account in calculating the stability of structures on the seabed. We explain the Morison equation, commonly used in calculating forces due to environmental loads underwater. Resisting force and moment and overturning moment terms are explained, as well as friction force and the values of static terms. Lastly in this chapter we explain what the breakdown of current loads is on the structure, and how this can be calculated.

In chapter 3.5.4 we detail the SUBFRAME calculator, its working principles and the choices made when calculating a structure. Limitations and future improvements will be explained.

In chapter 5 we give an overview of the modelled structures, and the resulting calculations that are output from the calculator. We compare this as well as possible to the real-life weather conditions.

Chapter 6 gives conclusions and recommendations for future development of the tool.

2.2 Case studies: Data collection of artificial structures

In this chapter we give an overview of structures, both artificial reefs and monitoring landers of various sizes that have been placed in the North Sea in the period 2020-2024. Knowledge on whether the structure is sanded, lost, what the weather was in the deployment time window and structure specifics are given in the table.

Table 1: Overview of deployed structures and their specifics

Project	Name	Sanded (s) or lost (l)?	Deployment duration [days]	Weather data available?	Stability calculation available?	Calculation condition	Dimensions LxWxH [m]	Weight (air) [kg]
Gemini	**Oysterspat collector**	**Yes (s)**	**449 (1); 435 (2); 418 (1)**	**yes**	**yes**	**1/1**	**2.0x2.0x0.5**	**35**
Gemini	Acoustic frames	no	199		yes	1/100	2.5x2.5x3.0	1500
Gemini	**MIXlander frame**	**no**	**199**	**yes**	**yes**		**3.5x2.5x1.5**	**1060**
Gemini	Measurement ladder	no	199		no	-		70
Gemini	Measurement ladder clump weight	no	199		no	-		200
Gemini	Measurement ladder chain	no	199		no	-	50m	110
Gemini	Oyster wireframes (external)	Yes (l)	Unk.	yes	no (afterwards)			15
Gemini	oyster shells	Yes (l)	~120		no		70x71x16.4 [mm]	0.1

Project	Name	Sanded (s) or lost (l)?	Deployment duration [days]	Weather data available?	Stability calculation available?	Calculation condition	Dimensions LxWxH [m]	Weight (air) [kg]
Offshore Test Site (OTS)	WERC dock	no	1736		yes		3.8x3.8x2.0	290
OTS	LUD cage + trees	Yes (s)	1736*	maybe	yes		2.5x3.2x0.9	477
OTS	**Arc Marine with steel top**	**no**	**1736**		**yes**		**1.5x1.0x1.5**	**1700**
OTS	Arc Marine Pyramid	no	1736		yes		1.5x1.0x1.5	1900

*The LUD cage moved approximately 500m during a first-year storm but has been stable for approximately two years now.

Three structures have been selected for further analysis, being the oyster spat collector, the Arc Marine cage with steel top and the MIXlander frame, indicated in the table in bold. They will be detailed in the subsequent chapters.

2.3 ARC Marine cage

The ARC Marine Reefcubes have a footprint of approximately 1.5 x 1.5m and a height of 1.75m. The structures are made of recycled materials with a density of 2350 kg/m3.
They were deployed at the Offshore Test Site, approximately 12km from the Scheveningen coast, at a water depth of around 21m. Subsequent surveys showed that the structures have been in place until at least August 2025, weathering various storms.

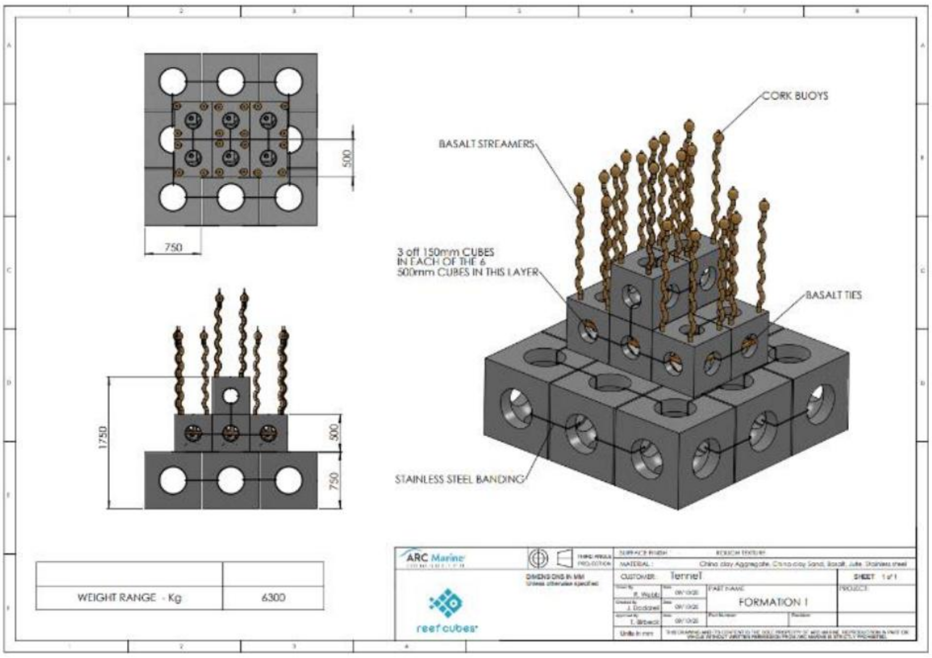

Figure 1: Schematic designs of ARC Marine Reefcube artificial reefs

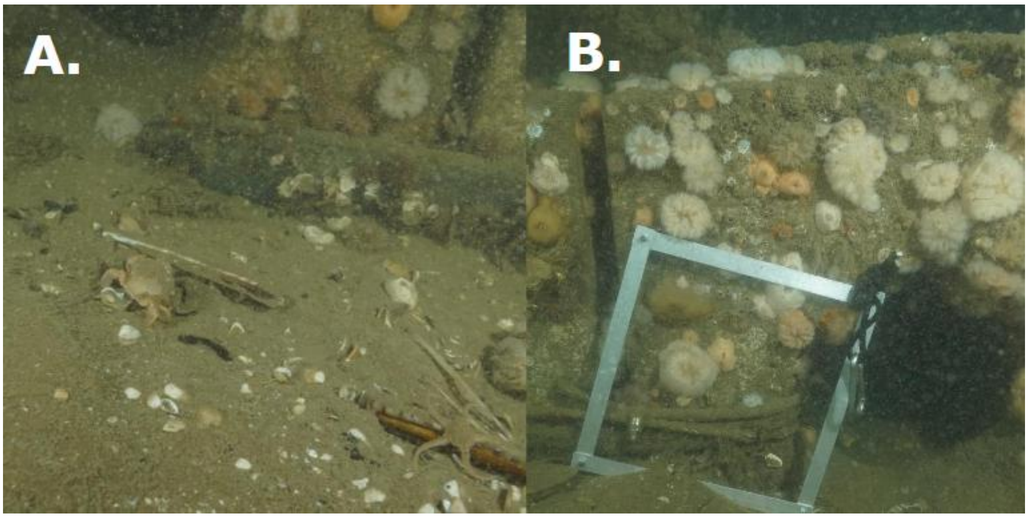

Figure 2: Marine life on deployed Reefcubes in the Offshore Test Site. Photos courtesy of Waardenburg Ecology BV.

Seaward

2.4 Oyster spat collector

A spat collector consists of a frame (see Figure 3), onto which four nets with shells are mounted (Pacific oyster shells or flat oyster shells, two with and two without BESE paste), and equipped with an acoustic release and a temperature datalogger. An ROV hook has been added to the frame as backup option for retrieval (Kamermans et al. 2024).
The frame weighs approximately 35 kg in air and is ~50cm high.

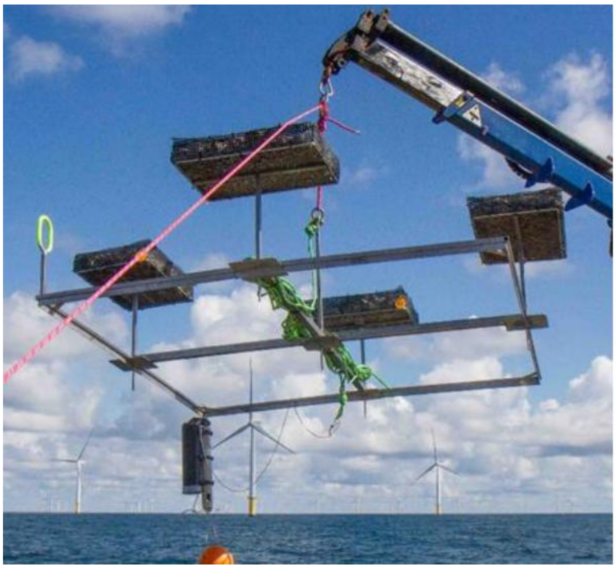

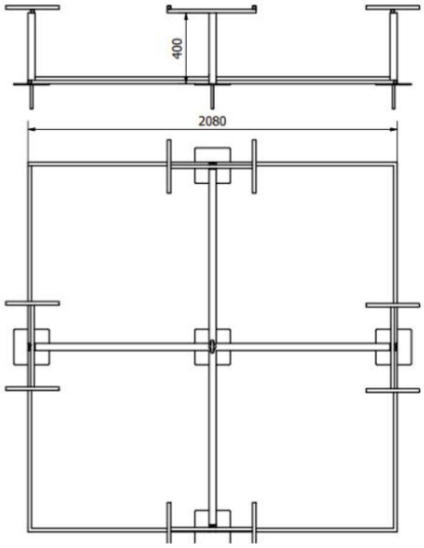

Figure 3: WINOR oyster spat collector frame. Left: during deployment. Right: technical drawing

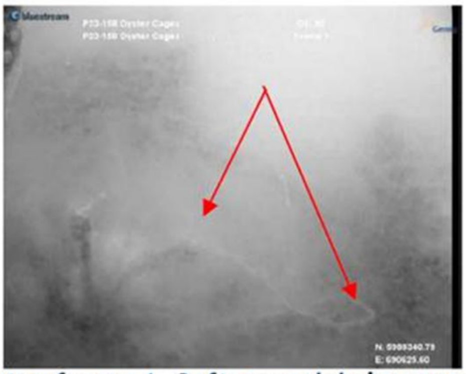

Oyster frame 1. Soft rope debris wrapped aropund multiple points of the frame.

Oyster frame 1, centre of the frame lifting ey

Figure 4: ROV screens of Frame #1 taken on 21-05-2024

During deployment in Q3 2023 the weather was characterized by long periods with a lot of wind and waves, and very few weather windows in which the wave height was less than 1m.

2.5 MIXLander frame

The MIXLander is a design made by NIOZ. An example of the structure is shown in Figure 5. The design allows near-bed measurements (Snoek 2021).

The dimensions of the MIXLander are as follows:

- Each corner has a foot with a collar to prevent sinkage into the surrounding bed
- The 4 feet are 2.47 m (maximum width at the seabed viewed from the front) and 2.28 m (maximum width as viewed from the side) apart from each other
- The appendages on the side of the structure increase the total maximum width (as viewed from the front) to 3.556 m
- The maximum height with respect to the seabed is 1.487 m.

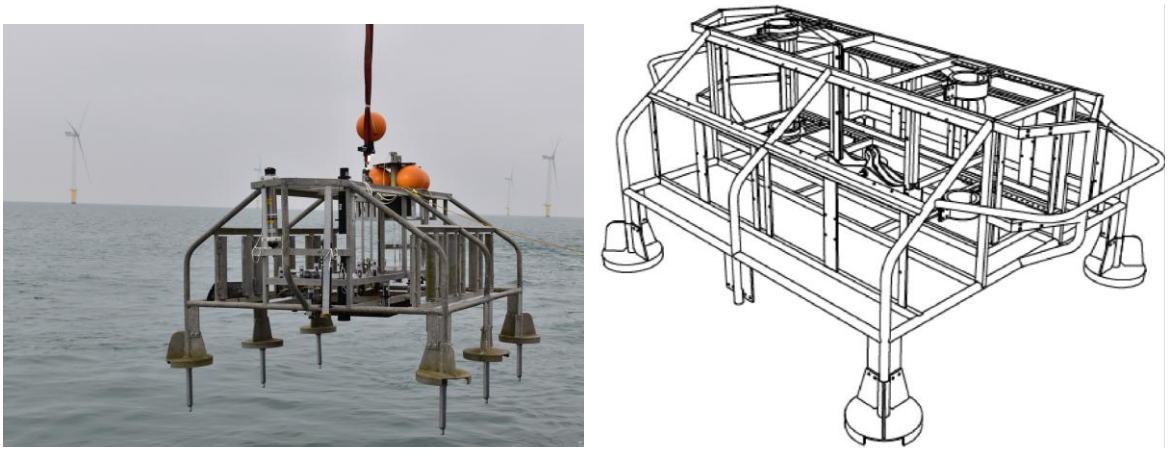

Figure 5: MIXLander frame. Left: during deployment. Right: technical drawing (first version).

Figure 6: Retrieval of MIXlander frame from Gemini OWF

Figure 7: ROV pictures of the feet of the MIXlander, 27-05-2023

3 Theoretical considerations

3.1 Introduction

In this chapter we will detail the governing equations used to calculate forces on the structure. We introduce and explain the Morison equation in chapter 3.2, detail the resisting force (friction force) and resisting overturning moment in chapter 3.3. These form the stability of the structure and stability is directly influenced by key parameters such as weight and size in parallel to current. Further, overturning moment and the current calculation are given in chapters 3.4 and 3.5 subsequently.
To ensure accurate forces over the structure height, the program discretizes the structure into 20 vertical slices. For each slice, the wave velocity, current velocity, and resulting forces are calculated and summed. A single-point calculation could under-, or overestimate forces based on structure design. In chapter 4.3.2 we calculated some cases to look at differences between discretization and single-point calculations.

3.2 Forces: Morison equation

When the currents are known we can use the Morison equation to calculate the forces on the structure. Refer to chapter 3.5 for the calculation of current.

The Morison equation forms the basis of the hydrodynamic model and calculates hydrodynamic forces on structures in oscillatory flow. The equation combines two force components: inertia force and drag force. The inertia term represents forces from water acceleration around the structure, proportional to fluid acceleration and structure volume.
The drag term accounts for viscous effects and flow separation, proportional to the square of fluid velocity.

The full Morison equation is expressed as (Morison et al. 1950):

$$F = \rho C_m V \dot{u} + \frac{1}{2} \rho C_d A u |u|$$

Where:

F	= total force on structure	[N]
ρ	= fluid density	[kg/m^3]
C_m	= inertia coefficient	[-]
V	= volume of the body	[m^3]
$\dot{u}$	= flow acceleration	[m/s^2]
C_d	= drag coefficient	[-]
A	= cross-sectional area of the body	[m^2]
u	= flow velocity	[m/s]

The inertia coefficient C_m typically ranges from 1.5 to 2.0 for circular cylinders, while the drag coefficient Cd ranges from 0.6 to 1.2. These coefficients depend on the Keulegan-Carpenter number and Reynolds number, determined through experiments or estimation. See Appendix A – Applicability criteria – Airy, KC and Reynolds numbers for more details about KC and Reynolds numbers.
In order to calculate the flow velocity, Airy wave theory can be applied, see chapter 3.5.2.

3.3 Resisting force and moment

Assuming a structure which is placed on the seabed the object has a certain weight that presses into the soil, resisting sliding movement. This is called friction force in the subsequent text.
Further, the object has a resisting moment against overturning due to its mass. The resisting forces and moments are explained in this chapter.

3.3.1 Friction force

First, we calculate the weight of the object when submerged:

$$W_{w,sub} = (\rho_{struc} - \rho_{water})\,Vg$$

Here

$W_{w,sub}$	= weight of submerged body	[N]
ρ_{struc}	= density of structure	[kg/m^3]
ρ_{water}	= density of seawater (1025)	[kg/m^3]
V	= volume of the body	[m^3]
g	= gravitational acceleration (9.81)	[m/s^2]

With a dynamic friction component, we calculate the sliding resistance force

$$F_{fric} = W_{w,sub}\,\mu_d$$

With

μ_d	= dynamic friction coefficient	[-]

The dynamic friction coefficient depends on the soil conditions, burial of the structure and grain size or shear stress of the soil.
DNVGL specifies generic dynamic friction coefficients as 0.6 on sand, 0.2 on clay and 0.6 on rock (*DNV-RP-F109: On-Bottom Stability Design of Submarine Pipelines* 2010). For a first approximation, these values will be used.

3.3.2 Resisting overturning moment

The structure has some resistance against overturning due to its mass. By using the moment arm (light blue line in Figure 8) and multiplying with $W_{w,sub}$ (black arrow) we can calculate the resistance to overturning moment M_{res}. Note that the overturning resistance will take place against the current direction (purple arrow).

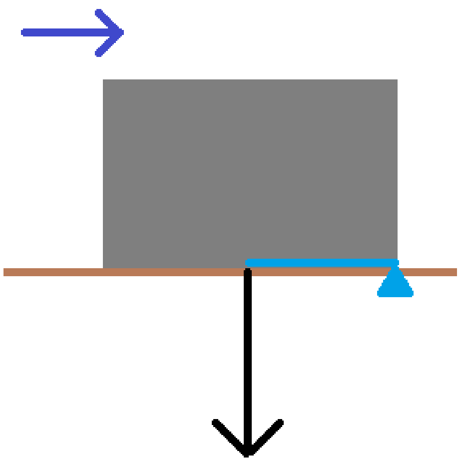

Figure 8: Resisting moment

$$M_{res} = 0.5\, W_{w,sub}\, d_{hor}$$

Where:

M_{res}	= resisting overturning moment	[Nm]
d_{hor}	= horizontal moment arm	[m]

The moment arm depends on the structure and needs to be calculated from the structure 3D file. Generally, for symmetrical structures the moment arm is ½ the length of the structure parallel to the current.

3.4 Overturning moment

Due to the currents and wave action on the structure the structure wants to overturn. We can calculate this overturning moment in various ways.
Two cases can be calculated:

- One is taking the average of the combined current and wave force, defined as environmental force F_{env} , at half of the structure height. This disregards the velocity profile that might be applied to the structure, see chapter 3.5.1. In chapter 4.3.2 a comparison between the two methods is given for an example structure.

Figure 9: Overturning moment, simple method

$$M_{OT} = 0.5\, F_{env}\, d_{ver}$$

Where:

M_{OT}	= overturning moment	[Nm]
F_{env}	= lateral combined current and wave force	[N]
d_{ver}	= vertical moment arm	[m]

- For the method implementing the current profile the overturning moment becomes a summation.

Figure 10: Overturning moment, discretized method

$$M_{OT} \approx \sum_i F_{env,i}\, d_{ver,i}$$

Where:

M_{OT}	= overturning moment	[Nm]
$F_{env,i}$	= lateral combined current and wave force applied at point (or slice) i	[N]
$d_{ver,i}$	= vertical lever arm from the pivot to the corresponding force	[m]

Seaward

3.5 Current calculation on the structure

Several hydrodynamic forces, and consequently moments, act on the structure.

- Steady current: A force arises from the mean current, which can be represented by a vertical velocity distribution such as the 1/7th power law.
- Wave-induced flow: Additional forces result from the oscillatory motion of waves. Attenuation factors may be introduced to account for energy dissipation with depth.

The combined flow field at depth is then represented as:

$$u_{total} = u_{current} + u_{wave}$$

With u_{total} known, the velocity component can be used in the Morison equation, see chapter 3.2, resulting in the forces on the structure due to steady current and wave-induced flow.

3.5.1 Steady currents

The current profile (1/7 power law) describes how the steady current varies with elevation above the seabed; it is a current profile. It takes the mean current speed and applies a factor dependant on depth according to the equation (Robert G Dean, Robert A Dalrymple 1991):

$$u_{current(z)} = \frac{8}{7} U_{mean} \left(\frac{z}{d}\right)^{\frac{1}{7}}$$

Where:

z	= local depth from the seabed	[m]
d	= maximum water depth	[m]
$u_{current(z)}$	= current speed as function of z	[m/s]
u_{mean}	= mean steady current speed	[m/s]

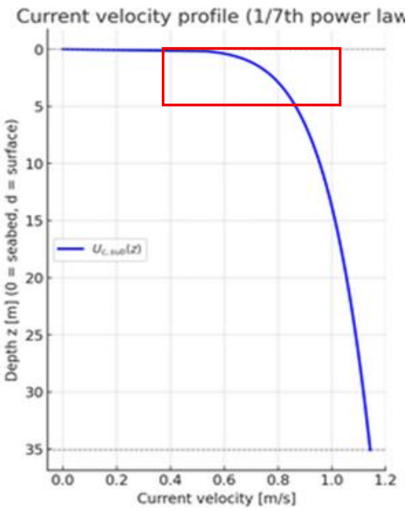

Figure 11: Example of a current velocity profile, courtesy of WaterProof. The seabed is y=0 so the typical range of velocities is indicated with the red square, for structures 0-5m in height.

3.5.2 Wave induced currents

Waves generate orbital motions that create clockwise circular currents in deep water. These orbital velocities change direction as waves pass, with water particles moving in the wave direction under wave crests and in the opposite direction under troughs. This cyclical motion creates circular paths in deep water, depicted in Figure 12.

With Airy theory (linear wave theory) these orbital velocities can be calculated if Airy wave theory can be applied. Application of Airy wave theory is dependent on such as water depth and wave heights, see Figure 13.

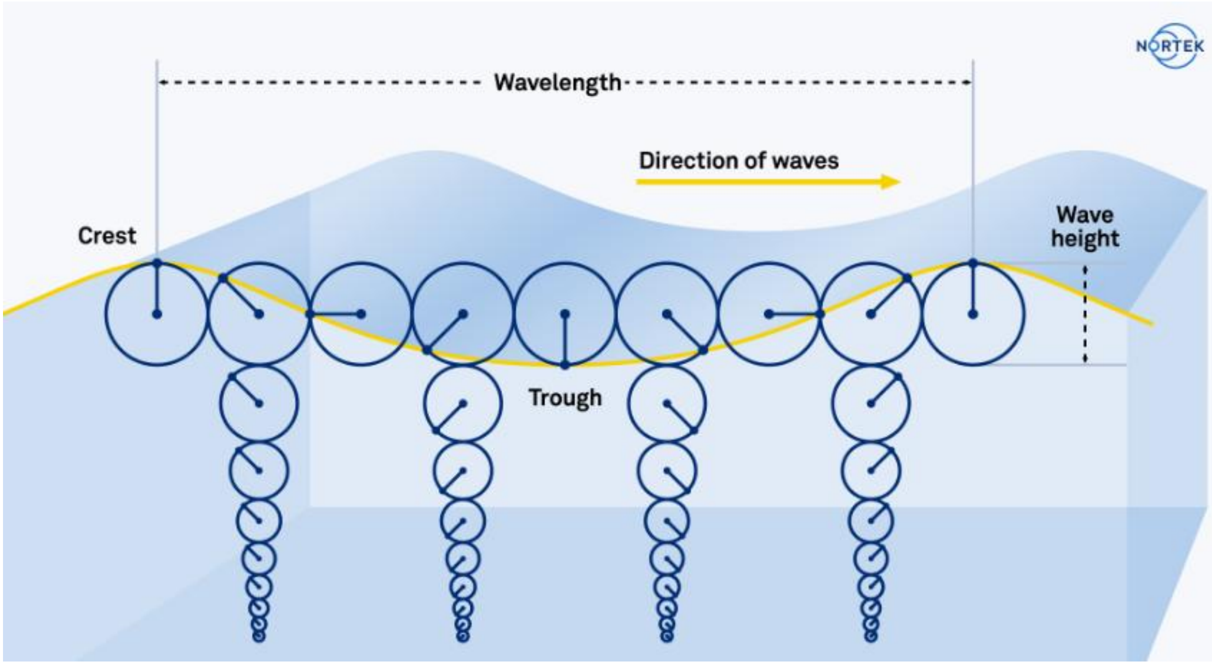

Figure 12: Description of orbital wave velocities attenuating with increasing water depth. (Nortek 2024; Nortek Support Cent. 2025)

The orbital wave velocity can be calculated using linear (Airy) wave theory if the requirements from Figure 13 are satisfied. The horizontal (u) and vertical (w) components of the particle velocity at a point (x,z) under a wave are given by:

$$u(x,z,t) = \frac{\pi H}{T}\frac{cosh\ k(z+d)}{sinh\ (kh)}cos(kx - \omega t)$$

$$w(x,z,t) = \frac{\pi H}{T}\frac{sinh\ k(z+d)}{sinh\ (kh)}sin(kx - \omega t)$$

With:

H = wave height

T = wave period

k = wave number

ω = $\frac{2\pi}{T}$ = angular frequency

h = water depth

Seaward

z = vertical position (positive upwards from seabed, z=0 at seabed, z=d at mean water level)
x = horizontal coordinate along wave propagation
t = time

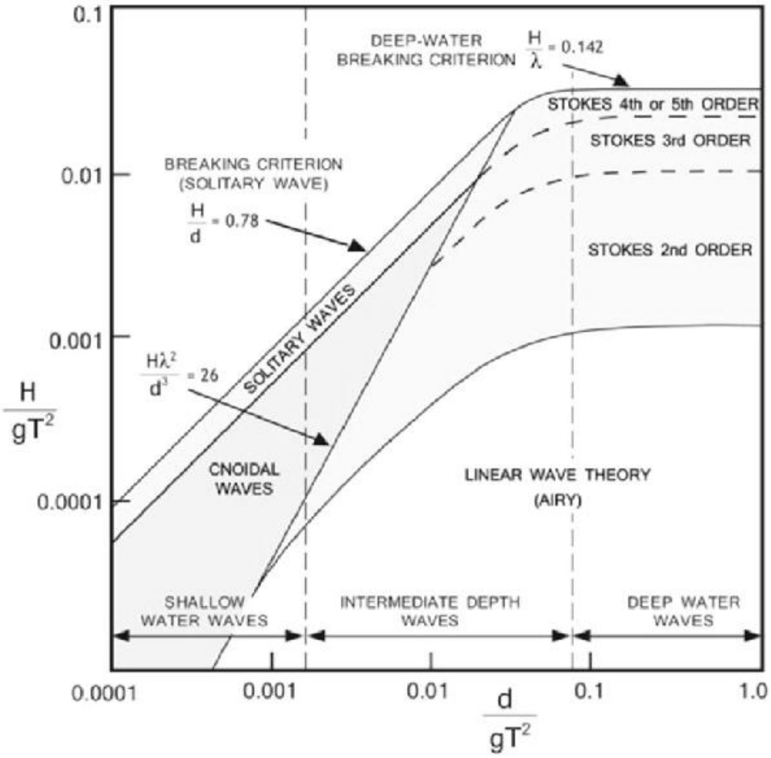

Figure 13: Airy wave applicability graph (Le Méhauté 1976). H is wave height, T is wave period, g is gravitational acceleration and d is local water depth

3.5.3 Dispersion relation

Airy wave theory assumes inviscid, irrotational flow and neglects energy dissipation during wave propagation. However, orbital velocities decay exponentially with depth, with attenuation more pronounced for shorter wavelengths. As a result, particle velocities and orbital excursions diminish with depth. Wave-induced motion therefore penetrates only to a finite depth, beyond which it becomes negligible. In deep water, short-period (high-frequency) waves do not generate measurable orbital velocities at the seabed, since their energy attenuates rapidly with depth.

The particle velocities predicted by Airy theory must therefore be interpreted as depth-dependent quantities subject to exponential decay. To quantify this attenuation, the dispersion relation must be solved to determine the wave number. The wave number *k* defines the spatial frequency of a wave and controls the vertical decay of orbital velocities in Airy wave theory:

$$k = \frac{2\pi}{L}$$

k = wave number [rad/m]
L = wavelength [m]

k can be obtained from the dispersion relation:

$$\omega^2 = gk\ tanh(kh)$$

This dispersion relation can be solved iteratively via Newton-Raphson iteration, fixed-point iteration or via approximations such as Hunt's for a given wave period and water depth (Fenton and McKee 1990; Hunt 1979). When testing the different methods using Dutch North Sea generally applicable values T_p = 8 s and a water depth of 27.0 m (intermediate depth):

Table 2: Dispersion relation calculation using different methods and Tp=8s, d=27.0m

Method	k (rad/m)	L (m)	Iterations	Calculation time
Hunt's approximation	0.06710	93.63	1 (direct)	Instant
Newton-Raphson	0.06710	93.63	2	Fast
Fixed-point	0.06710	93.63	7-8	Slower

For the sake of simplicity and computational speed Hunt's approximation and Newton-Raphson methodologies are deemed acceptable. Hunt's approximation might in some cases have a somewhat lower accuracy (0.1%) compared to Newton-Raphson (0.01%).

Hunt's approximation consists of the following equations:
Calculating the deep-water wavelength L_0:

$$L_0 = \frac{gT^2}{2\pi}$$

Here:
L_0 = deep water wavelength [m]

Then, when L_0 is known:

$$L = L_0 \, tanh\left[\left(\frac{2\pi d}{L_0}\right)^{0.75}\right]^{\frac{2}{3}}$$

With L we can calculate the wave number k in the previously given equation.
The wave number can then be used in the Airy wave equation.
An alternative is to use the iterative Newton-Raphson equation:

$$k = \left(\frac{\omega^2}{g}\right) \cdot \left(\frac{1}{\tanh(kd)}\right)$$

For values of $k_d < \frac{\pi}{10}$ shallow water is assumed. For $k_d > \pi$ deep water is assumed.
As a secondary check, d/L > 0.5 is assuming deep water where wave motion is negligible at seabed and hyperbolic functions can be simplified. At intermediate depth, 0.05 < d/L < 0.5 the full dispersion relation must be used. At shallow water, d/L <0.05 the wave speed depends on the water depth only, and wave motion extends to seabed.

Calculation checks for the example case in Table 2:
Since π/10 < kd < π (0.314 < 1.812 < 3.142), this confirms intermediate depth and thus the full dispersion relation must be used.
Also: d/L = 27/93.63 = 0.288 (between 0.05 and 0.5).

3.5.4 Significant and maximum wave heights

H_s and H_{max} are two different ways to express wave height:
The significant wave height H_s is defined as the mean of the top 1/3 waves in a given record (Nortek Support Cent. 2025). H_{max} is defined as the highest occurring single wave in the given sea sate('MetOcean Glossary', n.d.). In general $H_{max} \cong 1.86\ H_s$ (Bai and Bai 2014; 'MetOcean Glossary', n.d.)
In modelling reaction forces on a structure, a conservative approach will be to use H_{max} as wave height as this is the highest possible wave in the sea state. As input, H_s will be asked as this is often given in weather forecasting apps and programs. H_s will be converted to H_{max} and reaction forces, wave energy and other parameters will be calculated with this value as fundament.

4 The SUBFRAME calculator

4.1 Introduction

With the expert script as one of the research outputs we decided to program everything in the open-source programming language Python.

The program uses a Graphical User Interface (GUI) and STP/OBJ file loading.
It combines hydrodynamic force estimation under wave and current loading with structural stability checks, plots, and geometry-derived properties as described in chapter 3.
The application uses Airy wave theory and a 1/7th power-law current profile to calculate Morison's equation. The application has manual inputs for area, volume, centre of gravity, and mesh inspection.
See 4.1.2 for required Python libraries.

4.1.1 Morison

The Morison equation is applied at each time step to compute inertia and drag forces. Both force components receive a safety factor before summation into a force F_{total}. Friction is treated as a force derived from weight (see 3.3.1) multiplied by the friction coefficient.
Resisting moment is estimated using weight and a half-length moment arm.
Time dependent inertia, drag, force, and wave/current kinematics are visualised along with maximums of each force component. For calculation details, see chapter 3.

4.1.2 Required libraries

Base programming language is Python 3.13. Python can be expanded by loading libraries. Used libraries in the SUBFRAME calculator are as follows:

- numpy (>=1.20.0) - Numerical arrays and math operations
- matplotlib (>=3.3.0) - Plotting time series, velocity profiles, and heat maps
- PyQt5 (>=5.15.0) - GUI
- trimesh (>=3.10.0) - Loading and processing 3D models (OBJ, STL)
- scipy (>=1.7.0) - Generic scientific computing utilities
- parea (>=0.1.1) - Used for frontal area calculation for complex 3D structures
- numpy-stl (>=2.16.0) - STL file parsing and volume calculation for structure geometry
- gmsh (>=4.0.0) - Mesh generation and volume calculation for volume determination

Optional libraries (*EXPERIMENTAL FEATURES*):

- openpyxl - Excel export with formatted results and calculations
- reportlab - PDF export with plots and results

4.2 Input and output tabs

The calculator has four tabs: 3D Model Loader, Input Parameters, Results and Plots. Each tab will be described in the chapters below.

4.2.1 3D Model Loader

The 3D Model Loader is used to import the 3D files and create the visualization of the loaded file. It allows for rotation of axes in case these are not aligned correctly. A Structure Properties frame gives initial information about Centre of Gravity, mass (both dry and wet) and dimensions. Further info is given about the mesh (number of vertices, faces and whether or not the mesh is watertight). If the

model is correctly displayed and all values are in the correct order of magnitude, pressing the button Apply to Morison Calculation brings you to the next tab Input Parameters.
The loader attempts *trimesh* first, then falls back to a parser. COG calculations have safeguards: when vertex data is missing, the functions return None; with missing faces, the code falls back to averaging vertices. The COG therefore must always be checked thoroughly by the user, especially for complex structures.
The OBJ path can be auto-loaded when configured, but the program tracks the path and reuses it in calculations; missing files yield status messages.

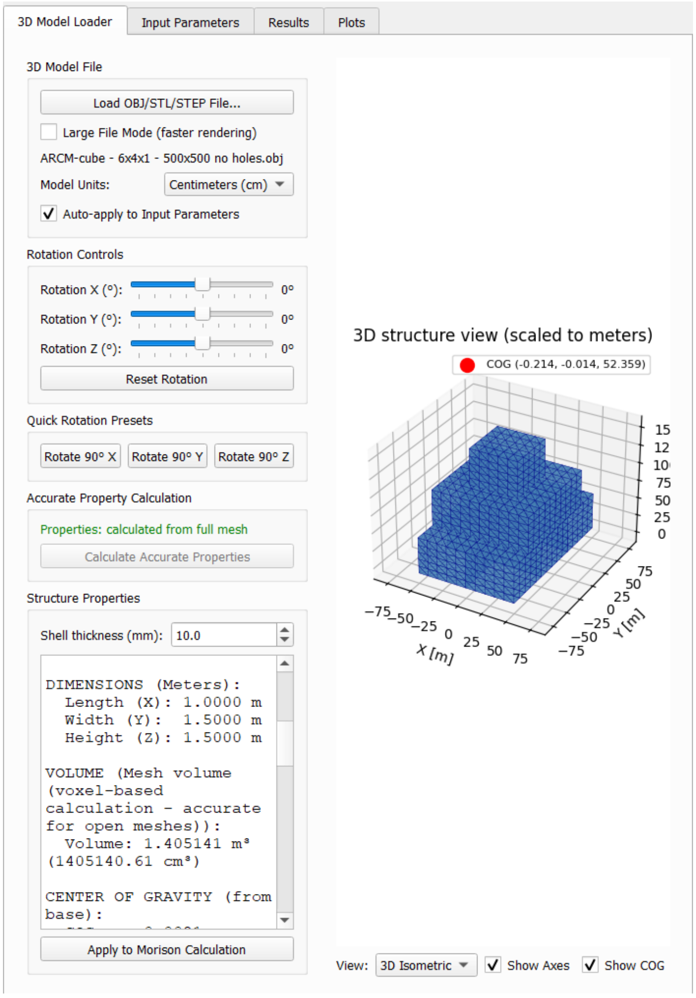

Figure 14: 3D Model Loader tab

4.2.2 Input parameters

The calculation process has an input function that uses various parameters (significant wave height *Hs*, period *Tp*, water depth *d*,), structure dimensions (*L, W, H)* and 3D Model Loader overrides (*Frontal area* and *Volume*), hydrodynamic coefficients (*Cm, Cd*), friction and safety factor, and densities. Lastly, current U_{mean} can be input by the user. See Figure 15.

The safety factor (sf) is applied to all calculated forces to provide a margin for uncertainties in the analysis method. The default value is 1.0, however typical design values range from 1.2 to 2.0.

The program determines a conservative wave height ($H_{max} = 1.86 \times H_s$) and wave number k via the dispersion relation, classifies water depth (deep, intermediate, shallow) using kd, and evaluates velocities and accelerations at the seabed with wave kinematics.
Current velocity profile uses the 1/7th power law over the structure height to produce velocities and an average. The velocity at each time step is the sum of wave-induced velocity and the current component.

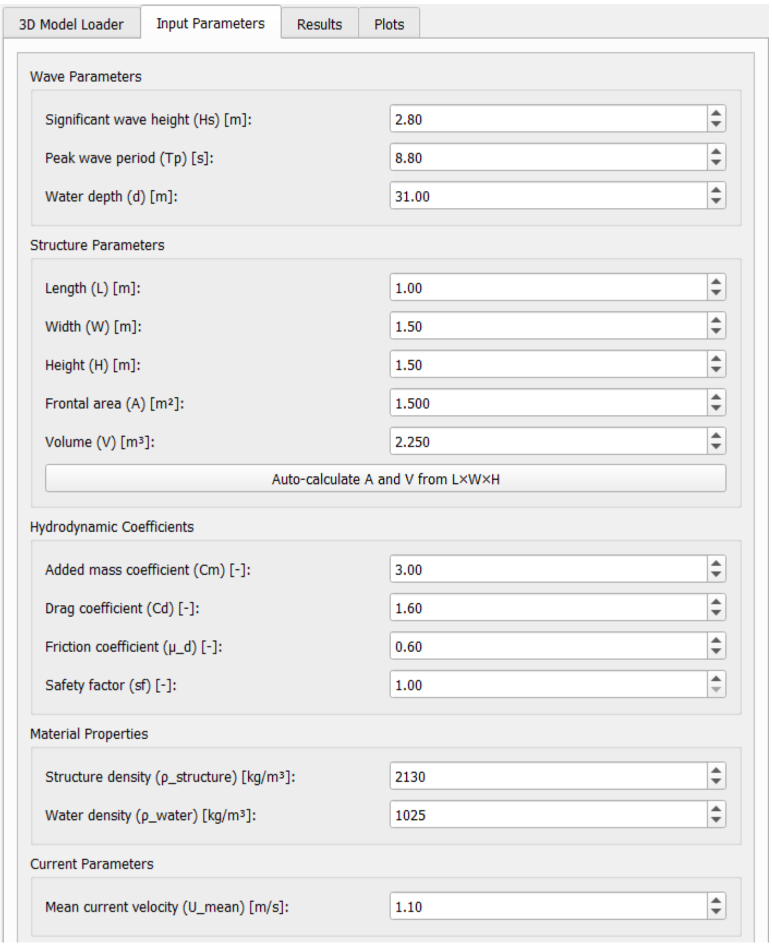

Figure 15: Input Parameter tab

4.2.3 Results

Results are presented as text and as plots.
The text results give all calculation steps used in the program. It gives intermediate results so the user can check results and find errors more easily. The format is in notepad style *".txt"* for easy copy-pasting into other programs or reports. Discretised currents, height of the structure and velocity components results are, for readability, not given per slice but rather summarized for highest, lowest and average value for the user to check. The resulting decomposition of forces is given as well as the resulting maximum force the structure will endure, given the phase shift included in the calculations. Lastly, theoretical safety factors are calculated by dividing the resisting (friction) force by the actual maximum force, and the same is done for the moment. An example result text is given in Figure 16.

```
================================================================================
MORISON FORCE CALCULATION RESULTS
================================================================================

WAVE PARAMETERS:
--------------------------------------------------------------------------------
Hs = 2.80 m (Significant wave height)
Tp = 8.80 s (Peak wave period)
d = 31.00 m (Water depth)

MAXIMUM WAVE HEIGHT:
--------------------------------------------------------------------------------
H_max = 1.86 × Hs = 1.86 × 2.80 = 5.21 m

WAVE NUMBER CALCULATION:
--------------------------------------------------------------------------------
ω = 2π/Tp = 2π/8.80 = 0.7140 rad/s
k = 0.055423 rad/m (from dispersion relation: ω² = g·k·tanh(k·d))
λ = 2π/k = 113.37 m (Wavelength)
k·d = 1.7181
Wave type: Intermediate water

STRUCTURE PARAMETERS:
--------------------------------------------------------------------------------
L = 1.00 m (Length)
W = 1.50 m (Width)
H = 1.50 m (Height)
A = 1.254 m² (Frontal area)
Volume = 1.405 m³
Mass = 2992.7 kg = 2.993 tonnes
ρ_structure = 2130 kg/m³

FRICTION FORCE CALCULATION:
--------------------------------------------------------------------------------
F_weight_submerged = (ρ_structure - ρ_water) × Volume × g
F_weight_submerged = (2130 - 1025) × 1.405 × 9.81
F_weight_submerged = 15230.27 N = 15.23 kN
F_friction = F_weight_submerged × μ_d = 15230.27 × 0.60
F_friction = 9138.16 N = 9.14 kN

CURRENT CALCULATION (Discretized over height):
--------------------------------------------------------------------------------
Current profile: Uc(z) = (8/7) × U_mean × (z/d)^(1/7)
Applied at each of 20 height slices:
  Uc at seabed (z=0):        0.0000 m/s
  Uc at center (z=H/2):      0.7442 m/s
  Uc at top (z=H):           0.8156 m/s
  Maximum Uc in structure:   0.8156 m/s

HEIGHT DISCRETIZATION:
--------------------------------------------------------------------------------
Structure discretized into 20 vertical slices
Height per slice: dz = 0.0789 m
A_slice = A / n_slices = 1.254 / 20 = 0.062700 m2
V_slice = V / n_slices = 1.405 / 20 = 0.070250 m3
Total A (sum of A_slice): 1.254 m2
Total V (sum of V_slice): 1.405 m3

APPLIED FORCE CALCULATIONS:
--------------------------------------------------------------------------------
Morison's equation: F = ρ × V × Cm × du/dt + 0.5 × ρ × A × Cd × u × |u|
Applied at each of 20 height slices and summed:
  Inertia term: F_inertia = Σ[ρ × V_slice × Cm × du/dt(z)]
  Drag term: F_drag = Σ[0.5 × ρ × A_slice × Cd × u_total(z) × |u_total(z)|]
  where u_total(z) = u_wave(z) + Uc(z) varies with height z
Safety factor applied: sf = 1.00
```

Figure 16: Results text after calculation

```
FORCE ANALYSIS:
--------------------------------------------------------------------------------
Maximum inertia force = 2.13 kN
Maximum drag force = 1.98 kN
Maximum applied force = 2.98 kN
Friction resistance = 9.14 kN (constant)
Time of maximum force = 7.467 s

MOMENT ANALYSIS (Overturning Stability):
--------------------------------------------------------------------------------
Overturning moment: M_overturn = Sum[F_slice × z_above_seabed]
  Maximum overturning moment = 2.35 kNm
  Time of maximum moment = 7.556 s
  Center of pressure (effective force height) = 0.788 m

Resisting moment: M_resist = F_weight_submerged × lever_arm
  F_weight_submerged = 15.23 kN
  COG source: OBJ file (trimesh)
  COG from OBJ: X=0.5000m, Y=0.7500m, Z=0.5227m
  (COG_y = lever arm for resisting moment, COG_z = height above base)
  Lever arm = 0.7500 m
  COG height = 0.5227 m above base
  Resisting moment = 11.42 kNm

MOMENT STABILITY:
  M_resisting / M_overturning = 4.86
  Structure is stable against overturning (ratio > 1.0)

VELOCITY COMPONENTS (Discretized):
--------------------------------------------------------------------------------
Wave velocity u_wave(z): varies from -0.6913 to 0.6917 m/s
  Average over structure height (at t_max): 0.4003 m/s
Current velocity Uc(z):  varies from 0.0000 to 0.8156 m/s
  Average over structure height: 0.6880 m/s
Total velocity u_total(z) = u_wave(z) + Uc(z)
  Average over structure height (at t_max): 1.0884 m/s
Maximum total velocity = 1.4341 m/s

SUMMARY:
--------------------------------------------------------------------------------
Structure: 1.0m x 1.5m x 1.5m, Mass: 2.99 tonnes

SLIDING STABILITY:
  Maximum applied force: 2.98 kN
  Friction resistance: 9.14 kN
  Sliding safety ratio: 3.06

OVERTURNING STABILITY:
  Maximum overturning moment: 2.35 kNm
  Resisting moment: 11.42 kNm (lever arm=0.750m)
  COG from OBJ: lever arm uses actual COG_y from trimesh
  Overturning safety ratio: 4.86

DETAILED SUMMARY VALUES:
--------------------------------------------------------------------------------
F_inertia = 2.13 kN
F_drag = 1.98 kN
F_total = 2.98 kN
F_friction = 9.14 kN
M_overturning = 2.35 kNm
M_stability = 11.42 kNm
SF moments = 4.86 (M_stability / M_overturning)
SF forces = 3.06 (F_friction / F_total)
================================================================================
```

4.2.4 Plots

The last tab is Plots, where the user finds 10 plots for their review, see Figure 17:

- Inertia force versus time over one complete wave period
- Drag forces versus time over one complete wave period
- Force comparison showing inertia, drag, and total forces together with the friction resistance line
- Bar chart summary of maximum forces, for quick comparison of force magnitudes
- Velocity profile over structure height at the time of maximum force, displaying wave velocity, current velocity, and total velocity components separately to detail relative contributions
- Velocity time series at different heights, showing how velocity varies both temporally and spatially.
- Small heat map showing total velocity as a function of depth and time
- Full-size heat maps showing wave acceleration and total flow velocity respectively, both displayed across the full water depth from surface to seabed as functions of time

Seaward

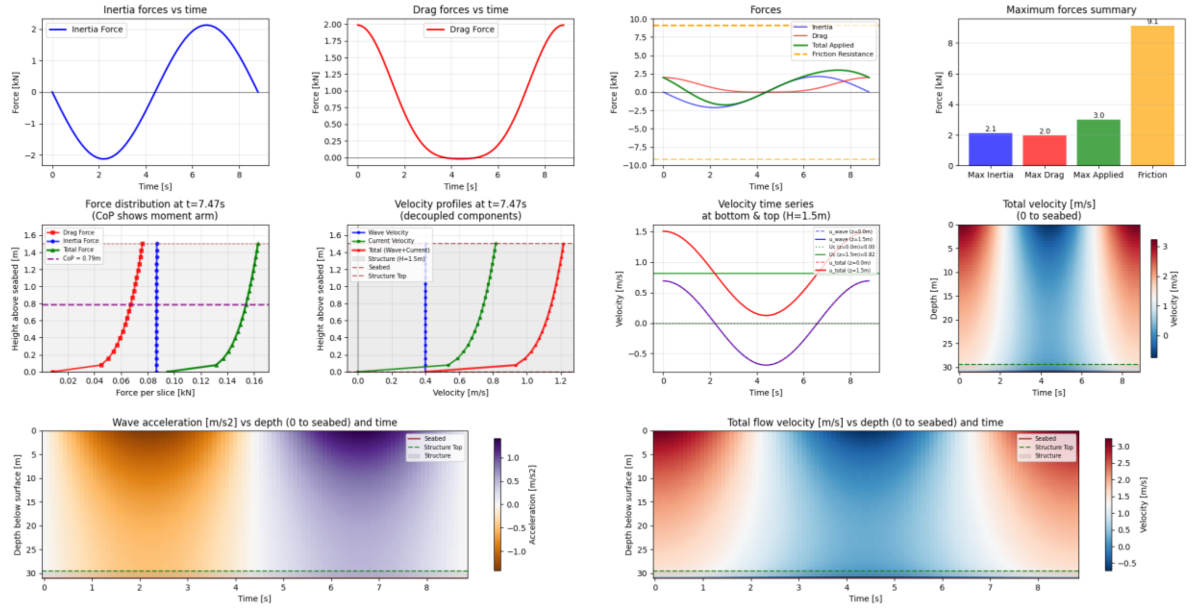

Figure 17: Plot output of the calculation program

4.3 Considerations during programming

The aim of this project is to also gain insights into the dos and don'ts of modelling stability for various structures.

4.3.1 Large files

During this process we contacted NIOZ to have a few more CAD drawings and test cases, which they provided. We are grateful to NIOZ for their assistance.
One of the things that came out of the NIOZ CAD drawings was that they are more detailed, and larger than the previous tested objects such as oyster spat collector (~3mb file) and ArcMarine structures (~10mb).
They provided us with a obj file of an experimental setup that was over 300mb. This caused the current file import method to slow down significantly when importing the file (~15min loading time on a Ryzen5 7640HS with 32Gb ram).
We have implemented a basic way using MeshLab to reduce the detailed mesh and thus reduce the file size and loading times of the file, with the cost of decreasing model accuracy.

For completeness the steps in MeshLab are as follows:

1. File → import mesh
2. Filters → Remeshing, Simplification and Reconstruction → Simplification: Clustering Decimation
3. Adjust and apply mesh specific settings
4. File → Export mesh as → Filename.obj

See chapter 5.3 for a comparison between the full and reduced mesh.

4.3.2 Discrete or single point currents

Averaging the currents by taking a single point on the structure from which to calculate: This is the simplest method and very fast. It calculates current forces at a single point (H/2) of the structure, or at the calculated COG from the loaded file. These heights, depending on structure design, do not have to be equal.

Discretization is a more accurate method:

- It slices the vertical structure height in 0.05m steps (d_z).
- At each step, it calculates the *local* wave kinematics and *local* current velocity.
- It calculates the force (dF) and moment (dM) on each slice (dA = W * dz, dV = L * W * dz).
- The total force $F_{(t)}$ and total overturning moment $M_{(t)}$ for each time step are the sum of all slice forces and moments.

4.3.3 Comparison of discrete and single point methods

Comparing the described methods of current calculation for the example 6x4x1 model.

Table 3: discrete vs single-point calculation comparison

	Case:	**1/2 of structure total height**	**Vertical COG as mid-point**	**Discretised over height**
Parameter	Unit	Single point	Single point	Discrete
U_{mean}	[m/s]	1.10		
$d_{max\ depth}$	[m]	35.1		
z (local depth above seabed)	[m]	0.75	0.52	n.a.
d_z	[m]	-	-	0.05
$U_{c,sub(z)}$=	**[m/s]**	**0.73**	**0.69**	**0.708**

Table 3 shows the single-point results and the discretised result. The discretised result was verified with calculations from WaterProof and shows *for this structure* taking the ½ structure total height gives an overestimation of structure current velocity, and taking the vertical COG as calculation height gives an underestimation of structure current velocity. Based on these results the discretised method is implemented as described in chapter 3.5, slightly sacrificing calculation speed for accuracy.

5 Evaluation of calculation method: Case studies (Object modelling)

The Morison equation assumes that both inertial and drag forces are significant, which is appropriate for larger structures in high-Reynolds-number flows.

5.1 ARC Marine equivalent structure modelling

A structure resembling the ARC Marine Reefcubes has been created in Fusion360. This model has been exported as an *obj* file and converted to *stl* with MeshLab.
A few variants have been created in order to test and finetune the program.

5.1.1 6 base, 4 mid, 1 top, without holes

Model consisting of 6 base blocks in 3x2 configuration, a middle layer consisting of 4 blocks in 2x2 configuration and one top block. All blocks are 500x500mm without holes/
Material density is concrete/stone at 2130 kg/m^3.

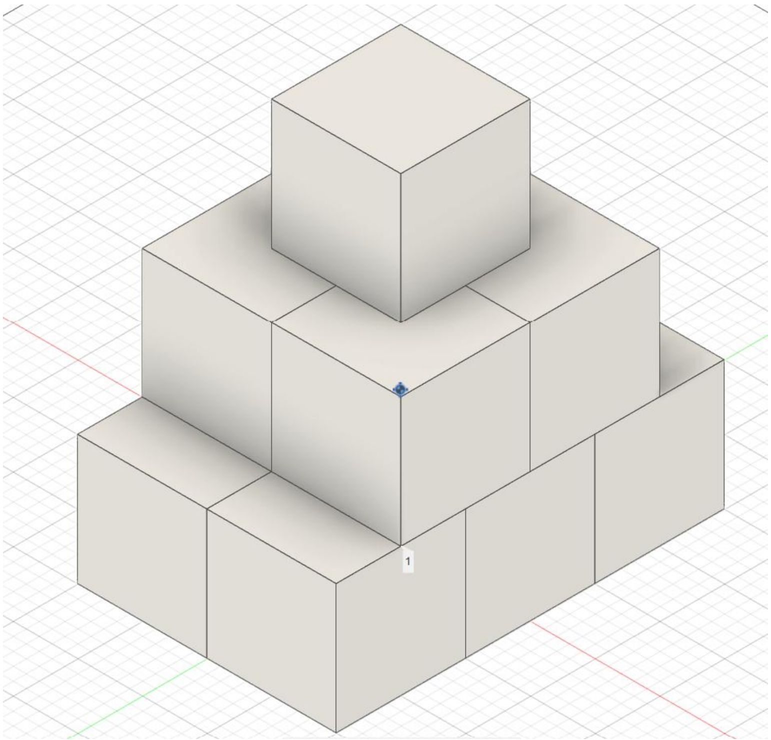

Figure 18: 6 base, 4 mid, 1 top, without holes 3D view

Table 4: 6 base, 4 mid, 1 top, without holes specifications

Configuration	Length / diameter [mm]	Width [mm]	Area [m^2]	# blocks [-]	Frontal area [m^2]	Volume [m^3]	Mass [kg]
2x2x1	500	500	0.25	5	1.25	1.375	2929
3x2x1				6	1.50		

CoG [XYZ] is : [-0.21, -0.01, 52.35] cm

5.1.2 6 base, 4 mid, 1 top, with holes

This model has the same block dimensions as the structure from 5.1.1.

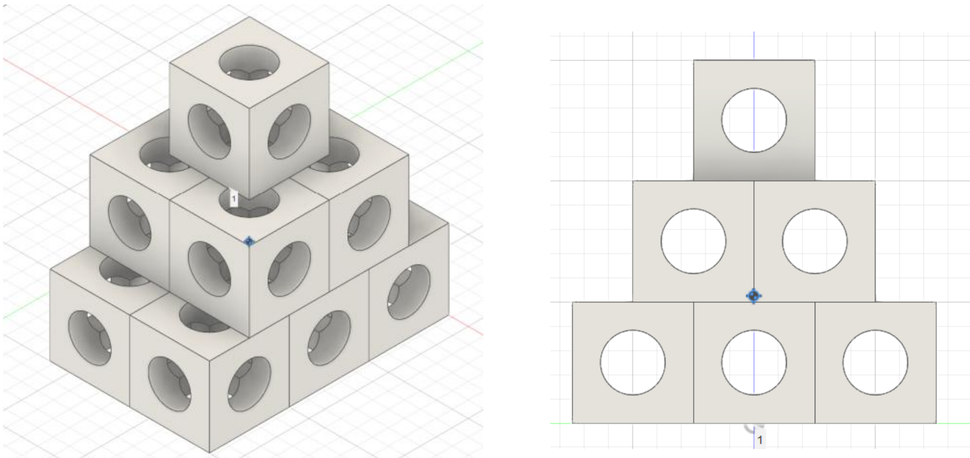

Figure 19: 6 base, 4 mid, 1 top, with holes 3D view and side view

CoG [XYZ] is : [-0.21, -0.01, 52.35] cm

5.2 Oyster spat collector model

Modelled in Inventor 2024 and imported via Fusion360 to be able to export it in a STL file. As the original file did not have a mesh, a simple mesh was applied to the model.
2440x2440x500mm, ~35kg in air.

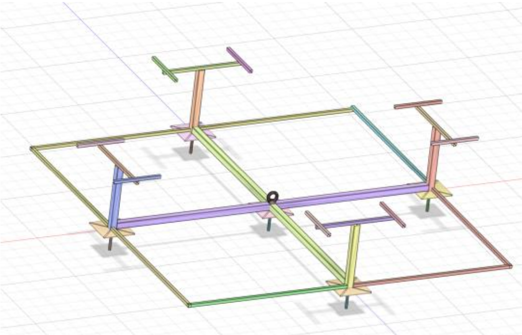

Figure 20: Oyster spat collector 3D model

Values used by Waterproof stability analysis (Luitze Perk 2023):

C_a	= 2.0	[-]
C_m	= 3.0	[-]
C_d	= 1.6	[-]
μ_d	= 0.6	[-]
a_2	= 1.0	[m]
ρ_{sw}	= 1025	[kg/m3]
g	= 9.81	[m/s^2]
sf	= 1.2	[-]
d	= 35.1	[m]
z	= 0.5	[m]

Where:

C_M	= inertia coefficient,
V	= volume of the structure,
a	= acceleration at the structure,
C_D	= drag coefficient,
A	= surface area that blocks the flow,
u	= flow velocities approaching the structure
a_2	= distance to turning point (1/2 length of structure parallel to flow)
sf	= safety factor
d	= water depth at location

5.3 MIXLander

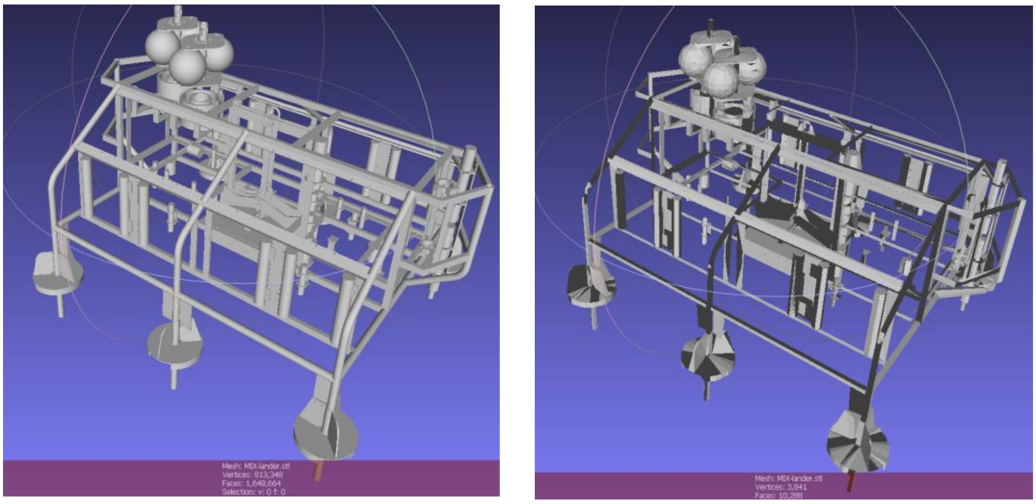

Figure 21: Mixlander frame, original mesh (l) and reduced mesh (r)

By reducing the mesh of the MIXLander frame we lose some detail; however the file size is reduced from ~80 Mb to 0.6 Mb, drastically improving loading speed. The difference in the object can be seen in Figure 21.

Dimensions:
Length (X): 3.2019 m
Width (Y): 2.6298 m
Height (Z): 2.4571 m
Volume: 0.12 m³
COG_x: 1.3092 m
COG_y: 0.0024 m
COG_z: 0.3691 m

Frontal area (Rasterization (accurate)):
A_xy (top view): 3.2564 m² (parallel to seabed)
A_xz (front view): 2.6170 m² (frontal to Y-direction)
A_yz (side view): 2.0958 m² (frontal to X-direction)

Mass estimation (using Input Parameters density: ρ=7800 kg/m³):
Mass in air: 969.52 kg (0.970 tonnes)
Buoyancy: 127.40 kg (seawater)
Submerged mass: 842.11 kg

5.4 Results and differences

5.4.1 Inputs

In Table 5 the inputs used for each model are given. In red are the manual adjustments made to the SUBFRAME calculator. It can be seen that the more complex a structure becomes, the more adjustment is needed, but this is only required for the volume mostly. Frontal area is often within 10% of the WaterProof number, depending on projection method (Voxel, Concave, Rasterization).

Table 5: Input case studies

#	Type	Inputs											
		Mass [kg]	Volume [m^3]	Frontal area [m^2]	Mat.density [kg/m^3]	Hs [m]	Tp [s]	Umean [m/s]	Water depth [m]	Ca [-]	Cm [-]	Mud [-]	Sf [-]
1	Arcmarine (solid)	2929	1.38	1.50	2130	2.80	8.80	1.10	31.00	2.0	3.0	0.6	1.5
2	Arcmarine (holes)	1592	0.75	1.16	2130	2.80	8.80	1.10	31.00	2.0	3.0	0.6	1.5
3	Mixlander (improved)	1060	0.16	2.35	6743	7.30	11.50	0.90	35.10	2.0	3.0	1.5	1.5
4	Oysterspat collector	43	0.01	0.27	3634	7.30	11.50	0.90	35.10	2.0	3.0	1.2	1.5
4.1	Oysterspat collector	43	0.01	0.27	3634	7.00	11.11	0.90	35.10	3.0	1.0	1.2	1.0

5.4.2 Results

In Table 6 the output results based on the input in Table 5 is given. As can be seen, results are generally in the order of magnitude compared to the calculations made by WaterProof.

Table 6: Output case studies

OUTPUT						
#	Type	Case	Fmor [N]	Fres [N]	Moverturn [Nm]	Mstab [Nm]
1	Arcmarine (solid)	WP calc	4416	-	7453	3243
		Auto loader SUBFRAME	4830	8940	7450	3840
2	Arcmarine (holes)	WP calc	3978	4860	4050	2799
		Manual adjustment SUBFRAME	3260	4880	4070	2630
3	Mixlander (improved)	WP calculation	22658	13227	11593	15638
		Manual adjustment SUBFRAME	23370	13460	11820	18210
4		WP calculation	3283	363	1233	315

OUTPUT						
#	Type	Case	Fmor [N]	Fres [N]	Moverturn [Nm]	Mstab [Nm]
	Oysterspat collector	Semi-Auto loader SUBFRAME - NO DETAILED MESH	2560	370	820	360
4.1	Oysterspat collector	WP calculation - no sf	1915	363	721	315
		Semi-Auto loader SUBFRAME - NO DETAILED MESH	1870	370	600	360

5.4.3 Differences

The differences between the WaterProof method (taken as the reference) and the SUBFRAME method (taken as the comparison) in percentage are given in Table 7. It can be seen that when manual adjustment of volume is carried out the SUBFRAME method generally comes within 20% of the WaterProof results, except for the overturning moment for the Mixlander prototype. This can be attributed to an unadjusted height; due to the design of the frame the calculation height becomes >2.5m, which greatly increases current influence. However, the COG is altered versus the reality due to the influence of the acoustic release floaters, as indicated in **Error! Reference source not found.**. D ue to the density of the material being uniform, the floaters have an unrealistically large influence on overturning moment.

Table 7: Procentual differences between WaterProof and SUBFRAME calculation methods

Differences in %						
#	Type	Casus	Fmor	Fres	Mresist	Moverturn
1	Arcmarine (solid)	Auto loader SUBFRAME	**9%**	**-**	**0%**	**18%**
2	Arcmarine (holes)	Manual adjustment SUBFRAME	**-18%**	**0%**	**0%**	**-6%**
3	Mixlander (improved)	Manual adjustment SUBFRAME	**3%**	**2%**	**2%**	**16%**
4	Oysterspat collector	Semi-Auto loader SUBFRAME - NO DETAILED MESH	**-22%**	**2%**	**-33%**	**14%**
4.1	Oysterspat collector	Semi-Auto loader SUBFRAME - NO DETAILED MESH	**-2%**	**2%**	**-17%**	**14%**

In general, taking 20% uncertainty margin gives a good estimate of structure performance. This uncertainty is lower with more simple and closed structures and increases with open structures. Especially the height estimation from the Autoloader, and thus the overturning moment is often too high calculated by the SUBFRAME calculator.

5.4.4 Weather analysis

For the MIXlander frame weather information from a nearby weather buoy was made available by Gemini.
On 23-11-23 at 21:45, during the time the MIXlander was on the seabed, the highest significant wave was recorded to be 11.4m Hs. Assuming a wave period of 12 seconds, we can assess whether the MIXlander should have been stable in these conditions.

Both Waterproof and the SUBFRAME calculator give at these values a safety factor of under 0.5, meaning that the forces and moments on the structures are almost twice as high as would be allowed.
However the structure has not been lost or moved so this might be an incidental high wave. To assess, we have experimented with T_p in the range of 8 – 20 seconds, and a H_s between 8 and 15 meter and carried out a Monte Carlo analysis with 300 calculations of the above cases, see Figure 22. From this graph, in this configuration it can be seen that both for sliding and overturning the Tp has a larger influence than the significant wave height. Further, there are some situations where the combination of Tp and Hs gives a safety factor > 1. Further analysis in the real-world situations might improve the calculation results; mainly better insight into the values as recorded by the buoy, and current speed (which was unknown).

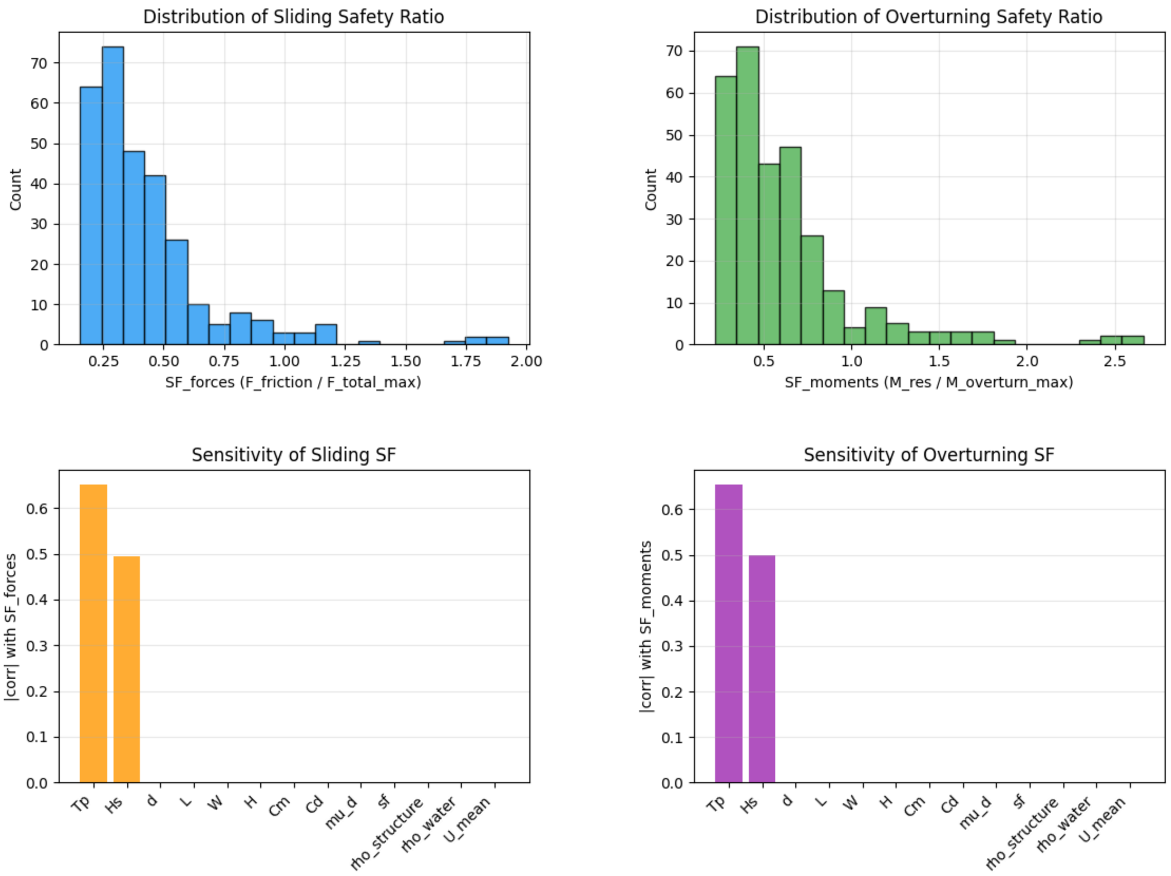

Figure 22: Experimental Monte Carlo analysis

5.5 Comparison of calculation methods

The method as described in the ECOFRIEND report (Bos et al. 2023) has been analysed and the following points of improvement are defined:

5.5.1 Frame

The Ecofriend method uses as input frames that are comprised of various cylindrical parts, summed together in the force and subsequent equations. This means that non-cylindrical frames, or frames consisting of non-cylindrical parts, cannot be analysed.

Proposed improvement

As almost all structures will nowadays have 3D CAD drawings from their design phase, a script that can load the structural 3D file into a Python environment is useful. This allows us to extract frontal area, centre of gravity (CoG) and volume automatically from the loaded 3D drawing. When we give a manual input for density, the structure can be fully defined and no extensive decomposition into subparts of the structure is required. This enables quicker analysis and is less prone to errors as it is based on calculation definitions.

5.5.2 Coefficient of friction

In the Ecofriend method a static coefficient of friction is defined. This is a fast way to obtain the friction force of the structure and sufficient for a first estimation. However, an estimation friction factor does not take into account soil dynamics such as shear. In this stage of programming and tooling, an experimental soil pressure model is used based on a simplified model where allowable soil pressure is an input and the weight and contact area of the loaded object is acting pressure.

Proposed future improvement

There are soil shear guidelines from both DNVGL and ABS (P. Jeanjean; F.G. Watson; H.J. Kolk; S. Lacasse 2010; *DNV-RP-F109: On-Bottom Stability Design of Submarine Pipelines* 2010) used in the oil and gas industry. When implementing these methods, we can model soil shear physics models.

5.5.3 Movement of structure

In the Ecofriend report, the movement of the structure is calculated by taking a particle and calculating its position due to currents every 10 minutes. This is done for a particle that follows the water motion perfectly. Implemented is the displacement only when the overturning or sliding force exceeds the structure friction force or resisting overturning moment. Second order displacement effects due to Stokes' drift are calculated to be negligible. The number of waves every 10-minute intervals is obtained by dividing 600 seconds (10 minute intervals) by T_p. The probability of exceedance of a reference wave is computed using a Rayleigh distribution. Finally, a reduction factor is defined to account for mass (inertia) and buoyancy effects of a larger structure compared to the particle. This factor can be obtained with scale tests.

Remark with respect to movement

The above methodology focusses to assess whether a not a structure is likely to be displaced. For the sake of practical simplicity, in this project we will only consider whether or not the forces or moments on the structure will be exceeded. If the calculation shows that the structure will be displaced, the design must be altered.

Further, when calculation methodologies proved insufficiently in line with the real world, and although sufficient stability was calculated but the frame has been lost or moved anyway, any pathway search will likely prove futile, as most structures will probably be placed in remote offshore locations, only visited once or twice per year. Hence, if a storm occurs, it is not feasible to directly check whether the frame is still at the outplaced location. When time passes, the frame might move even further from the intended location, with exceedingly divergent pathways compared to the models. Therefore, we aim to keep it simple: If a structure is found to be displaced: get recent storm information and direction, and start looking in that direction onwards as a starting point.

6 Conclusions & Recommendations

6.1 Conclusions

A calculation tool was developed to make quick design iterations possible for underwater structures and their stability. The tool, using Python software, is assumed to offer stability results within 20% of a detailed calculation. In general, taking 20% uncertainty margin gives a good estimate of structure performance. This uncertainty is lower with more simple and closed structures and increases with open structures.

The tool is constructed based on the Morison equations, uses linear wave theory (Airy waves) and can load simple or reduced mesh 3D objects for quick iterations. Further, the report details design considerations such as discrete and singe point current calculation methods.

A comparison is made with the methodologies used by WaterProof, which works on a case-by-case basis, and the calculation methodology applied to the ECOFRIEND project. In general, the SUBFRAME methodology proposed here gives good order-of-magnitude results and can be improved to have more options, calculation options and output options.

Main improvement points would be the manual override setting on every calculated value, such as COG. faster 3D mesh loading, as the tool now requires either long wait times or a reduced (simplified) mesh and saving of a calculation.

Additional functionality may be programmed in the future, such as the option for Monte Carlo simulations giving detailed limits of the structure in various conditions, and the option to compare more designs with each other in terms of stability. Steps were made in this regard but in order to validate the methodologies a follow-up project might be considered.

This calculation tool as of now is a first step into a complete software which ultimately might be used for quick iterations, is validated and verified, and accepted by e.g. wind farm operators as it is based on first-principle calculation bases.

6.2 Recommendation guidelines for tool use

It is recommended to always perform a detailed calculation for a final design check on stability.
The tool can be improved according to the recommendations in Chapter 6.3.

We recommend continuing the improvement of this tool as it shows promise for a robust kind of simulation software which can be useful for laypersons to help in preliminary design iterations.

Specific recommendations for the Nature Regeneration North Sea programme:

1) Implement a decision framework: use SUBFRAME calculations for preliminary conceptual design then validate critical cases with detailed analyses when final geometry is available.
2) Prioritize WaterProof methodology for final designs, or complex structures or complex flow interactions or when designing on the limit (output safety factor approaches or is below 1.0)
3) Recognize SUBFRAME limitations: SUBFRAME is effective for detailed force predictions on geometries. However, SUBFRAME struggles with complex meshes and designs.
4) Always cross-validate methods, conduct sensitivity analyses on drag/inertia coefficients, and maintain safety factors of ≥2.0 for overturning stability. Do not rely on single calculation methods for final design approval and always check the impact of volume/frontal area ratios

on prediction accuracy or extrapolate SUBFRAME results beyond validated geometry ranges without physical testing.

5) Flume testing: If project budgeting allows, conduct flume tests to validate initial predictions and refine Morison coefficients. While this increases upfront costs, model testing provides surer data on hydrodynamic behavior, reduces design margins through improved confidence, identifies unforeseen failure modes, and can prevent under- or overengineering. Flume tests are particularly useful when the Morison equation assumptions (small structure relative to wavelength, linear wave theory applicability) may be violated or when operating in the transitional regime between drag-dominated and inertia-dominated responses.

6.3 Recommendations

- Main improvement points would be the manual override setting on every calculated value, such as COG.
- Faster (full) 3D mesh loading, as the tool now requires either long wait times or a reduced (simplified) mesh and saving of a calculation.

Additional functionality may be programmed in the future, such as:

- The option for Monte Carlo simulations giving detailed limits of the structure in various conditions by the user giving a range of conditions and let the program run hundreds or thousands of cases with for example varying wave height, peak period, current velocity and water depth based on probability distributions. This results in specific conditions the structure becomes unstable, rather than the current single ‘in situ’ approach. The output would indicate: "The structure has a x% probability of stability at Hs < 3.2 m" or "y% failure risk under combined conditions of Hs > 6 m and Umean > 1.2 m/s".
- Monte Carlo simulations, but now for the inputted design varying frontal area, volume, material density and maybe soil mechanics. Intelligent decision trees could be implemented, where a user inputs a preliminary design, calculations are made and based on the calculations improvements that make the structure stable are proposed. For example: “The structure is at it current design not stable due to the friction factor being too low. When 10cm pins are added below the feet, the structure will be stable for the given conditions”.
- The option to compare multiple designs directly with each other in terms of stability.
- Add factoring or calculation for sliding resistance, especially with feet or pins pushed into the seabed (e.g. the MIXlander frame). Current calculations focus on overturning stability and hydrodynamic forces and summarize soil mechanics into a generic factor, hereby neglecting the actual contribution of soil mechanics to overall stability. Implementation of sliding resistance calculations provides a more complete picture of stability margins. This can be done applying methodologies based on ABS and DNVGL.
- Inisghts into the static factors that can be applied and what their overall influence is on the results.
- Quality of life improvements:
    - Improved visualization and results
    - Better reporting (bug/error free)
    - Saving and loading of previous calculations
    - Saving of mesh/data for quick loading next time
    - Automatically simplifying mesh
- Providing a web-based service to be able to share the tool widely with stakeholders and interested parties.

7 Bibliography

Bai, Qiang, and Yong Bai. 2014. '7 - Hydrodynamics around Pipes'. In *Subsea Pipeline Design, Analysis, and Installation*, edited by Qiang Bai and Yong Bai. Gulf Professional Publishing. https://doi.org/10.1016/B978-0-12-386888-6.00007-9.

Bos, Oscar G., Pauline Kamermans, Linda Tonk, et al. 2023. *Eco-Friendly Reef Restoration Pilots in Offshore Wind Farms: Report Project ECOFRIEND 2019-2023*. June. https://doi.org/10.18174/632058.

DNV-RP-C205: Environmental Conditions and Environmental Loads. 2010.

DNV-RP-F109: On-Bottom Stability Design of Submarine Pipelines. 2010.

EngineerExcel. 2025. 'What Does Reynolds Number Represent?' *EngineerExcel*, January 25. https://engineerexcel.com/what-does-reynolds-number-represent/.

Fenton, J. D., and W. D. McKee. 1990. 'On Calculating the Lengths of Water Waves'. *Coastal Engineering* 14 (6): 499–513. https://doi.org/10.1016/0378-3839(90)90032-R.

Hunt, John N. 1979. 'Direct Solution of Wave Dispersion Equation'. *Journal of the Waterway, Port, Coastal and Ocean Division* 105 (4): 457–59. https://doi.org/10.1061/JWPCDX.0000168.

Kamermans, Pauline, Oscar Bos, Edwin Kardinaal, and Nathanael Gelwynse. 2024. *WINOR Oyster Spat Collection Experiment in Wind Park Gemini Zee-Energie*. Wageningen Marine Research. https://doi.org/10.18174/669522.

Le Méhauté, Bernard. 1976. 'Inertia Forces'. In *An Introduction to Hydrodynamics and Water Waves*, edited by Bernard Le Méhauté. Springer. https://doi.org/10.1007/978-3-642-85567-2_4.

Luitze Perk. 2023. 'Stability Assessment Oysterspat Collector'. Memo. June 7.

'MetOcean Glossary'. n.d. Accessed 23 September 2025. https://glossary.metocean.co.nz/?maximum-wave-height.

Morison, J. R., J. W. Johnson, and S. A. Schaaf. 1950. 'The Force Exerted by Surface Waves on Piles'. *Journal of Petroleum Technology* 2 (05): 149–54. https://doi.org/10.2118/950149-G.

Nortek. 2024. *Principles of Operation - Waves*.

Nortek Support Center. 2025. 'What Is the Difference between Hm0 and Hs?' January 7. https://support.nortekgroup.com/hc/en-us/articles/360029507012-What-is-the-difference-between-Hm0-and-Hs.

P. Jeanjean; F.G. Watson; H.J. Kolk; S. Lacasse. 2010. *RP 2GEO: The New API Recommended Practice for Geotechnical Engineering*. 903–8. https://doi.org/10.1201/b10132-135.

Robert G Dean, Robert A Dalrymple. 1991. *Water Wave Mechanics for Engineers and Scientists*. Vol. 2. Advanced Series on Ocean Engineering. https://www.worldscientific.com/worldscibooks/10.1142/1232.

Snoek, Roelant. 2021. *Stability Assessment NIOZ MIXLander Frame*. Memo WP1220_R1r0. Waterproof.

Appendix A – Applicability criteria – Airy, KC and Reynolds numbers

Practical application limits for Airy, Keulegan-Carpenter and Reynolds numbers along with their definitions and explanations are given in this chapter.

Airy wave theory

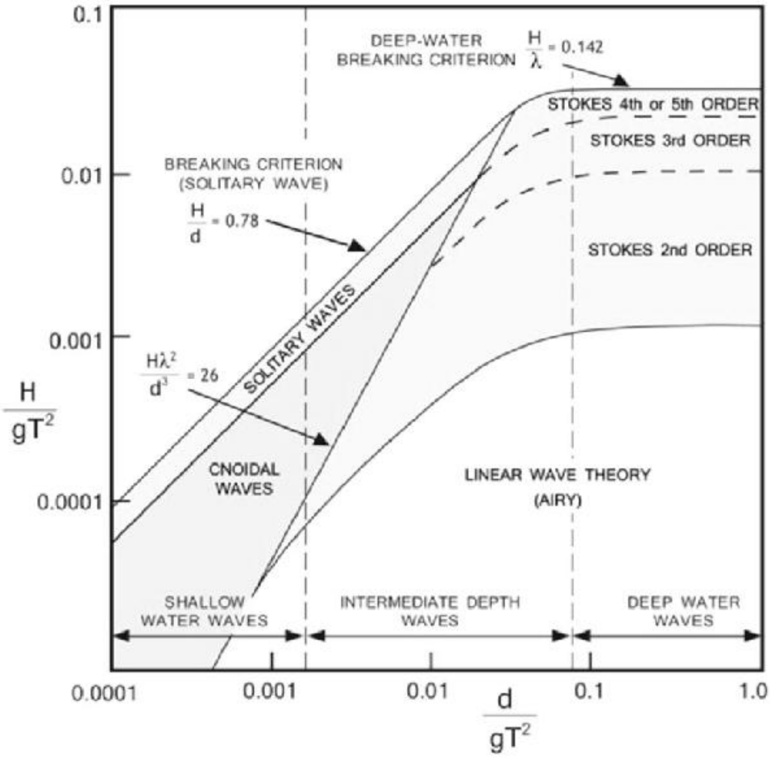

Figure 23: Airy wave applicability graph (Le Méhauté 1976). H is wave height, T is wave period, g is gravitational acceleration and d is local water depth

Keulegan-Carpenter number

The Keulegan-Carpenter (KC) number represents the ratio of fluid displacement to structure diameter.

$$K_c = \frac{VT}{L}$$

Where:

V	= amplitude of the flow velocity oscillation	[m/s]
T	= oscillation period	[s]
L	= characteristic length scale	[m]

For actual implementation of KC numbers the reader is referred to (*DNV-RP-C205: Environmental Conditions and Environmental Loads* 2010) par 6.7 where a framework is given based on surface roughness and appropriate KC number calculation methodologies.

Reynolds number

Reynolds number characterizes flow regime around the structure.

$$Re = \frac{\rho u L}{\mu}$$

Where:

ρ	= fluid density	[kg/m^3]
u	= flow velocity	[m/s]
L	= characteristic length scale	[m]
μ	= dynamic viscosity of the fluid	[kg/(m·s)]

Reynolds number for laminar flow

The laminar flow regime generally occurs at Reynolds numbers ranging from 0 to 10^3. At Reynolds numbers between 0 and 1, the flow is highly viscous and characterized by a creeping motion. Between 1 and 10^2, the flow is still laminar and strongly dependent on the Reynolds number.

When fluid flows over a solid object the molecules in the fluid interact with the surface, resulting in the formation of a thin layer of fluid adjacent to the solid surface.

Reynolds number for transitional flow

The transition region between laminar and turbulent flows occurs in the range of 10^3 and 10^4. Engineers generally avoid designing flow operations in this region because of its unpredictable nature.

Reynolds number for turbulent flow

Generally, the turbulent flow regime occurs at Reynolds numbers in the range of 10^4 and above. Within the range of Reynolds numbers between 10^4 and 10^6, the flow characteristics are still moderately influenced by the value of Reynolds number. (EngineerExcel 2025)
For high Reynolds numbers, the impact of viscosity on the flow will be very small because the impact of viscosity on the flow relative to inertia is very small. Therefore, the flow can be modelled as inviscid.

In the calculator Reynolds is assumed to be turbulent. The Reynolds regime affects the Morison equation through C_{DS}, which feeds into C_D via the wake amplification factor ψ (KC). For more information on this, refer to (*DNV-RP-C205: Environmental Conditions and Environmental Loads* 2010) par 6.7 and figure 6.4 in that document.

Appendix B – Background on ocean wave terminology

Ocean waves are created by various forces that disturb water surfaces, including gravitational effects, weather and vessel wakes. Once formed, waves carry massive amounts of energy across water bodies.

Terminology of waves

We can describe waves using sinusoidal functions, which allows for analysis of wave characteristics (Nortek 2024). For basic wave parameters see Figure 24. Parameters used are mean sea level or still water level, crest and trough, wave height (the vertical distance between crest and trough), wavelength (distance of one complete wave cycle), amplitude (half the wave height), direction of propagation, wave period (time between successive peaks or crests), and wave frequency (inverse of wave period).

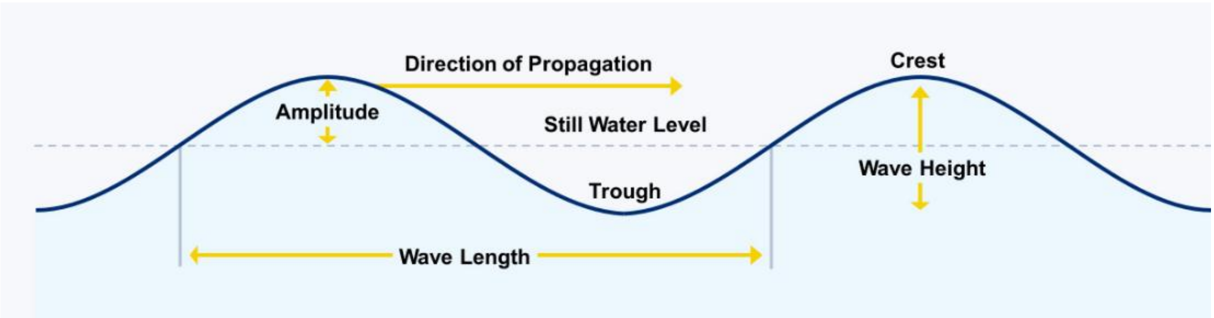

Figure 24: Basic wave parameters

As stated, waves carry plenty of energy. However, the wave energy distribution varies considerably across different time scales. Wind-generated waves form when energy transfers from wind to the water surface, creating circular water motion that doesn't advance with the wave itself. Local wave environments typically combine local wind waves with long-period swell generated by distant storm events, resulting in complex wave fields with different amplitudes, periods, and directions.

Wave classification depends on water depth relative to wavelength. Deep water waves occur when total water depth exceeds half the wavelength, producing circular orbital motion that diminishes with depth. Shallow water waves occur when depth is less than one-twentieth of wavelength, creating elliptical surface motion that flattens progressively with depth until becoming strictly horizontal at the bottom. Transitional waves occur between these depth ranges. For the North Sea region and throughout this report, deep water waves are assumed.

Wave spectra

General wave spectra are made up of waves with various amplitudes, wave heights and wave lengths. A wave spectrum describes the distribution of wave energy across frequencies, representing sea states statistically. It defines how wave energy varies with frequency and direction, with models like Pierson–Moskowitz or JONSWAP used to characterize wind-generated seas and compute responses of structures to irregular waves. In current stability analysis methods, single waves are used as an input into the model. It might be interesting to see what a full spectrum will give as a resulting stability output.

Dynamic pressure

Dynamic pressure represents another subsurface property, reaching maximum values under wave crests and following predictable attenuation patterns with depth and wavelength. Linear wave theory models this attenuation behavior.

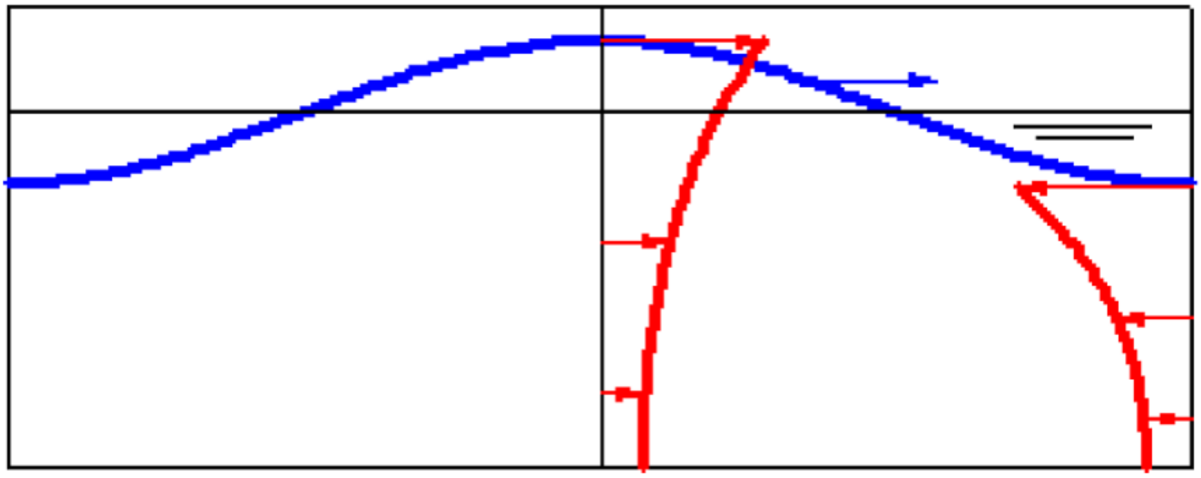

Figure 25: A wave moves in the direction of the blue arrow. The pressure profile is shown in red. (Nortek 2024)

Since sea surfaces consist of irregular combinations of different wave types varying in time and space, wave characterization requires statistical analysis. Two fundamental assumptions enable this approach: the wave field can be described as a summation of sine waves with different frequencies, amplitudes, and directions, allowing Fourier analysis application; and the wave field remains statistically stable over short measurement periods.

Time series analysis provides the most intuitive method for estimating wave parameters by evaluating sea surface displacement sequences over specified time periods. The zero-crossing method identifies individual waves where traces cross the mean water level, determining wave heights and periods for each wave in the record. Individual waves can then be ranked by height and period to calculate common statistical estimates.